

7.1) Introduction

Arrayed waveguide gratings (AWGs) are highly integrated moving average (MA) filters that are used for multiplexing and demultiplexing channels. They are capable of increasing the aggregate transmission capacity of a single-strand optical fibre [1]. Other names for these devices include waveguide grating routers (WGRs) and phased arrays (PHASARs). A schematic representation of the layout is presented in figure 7.1.

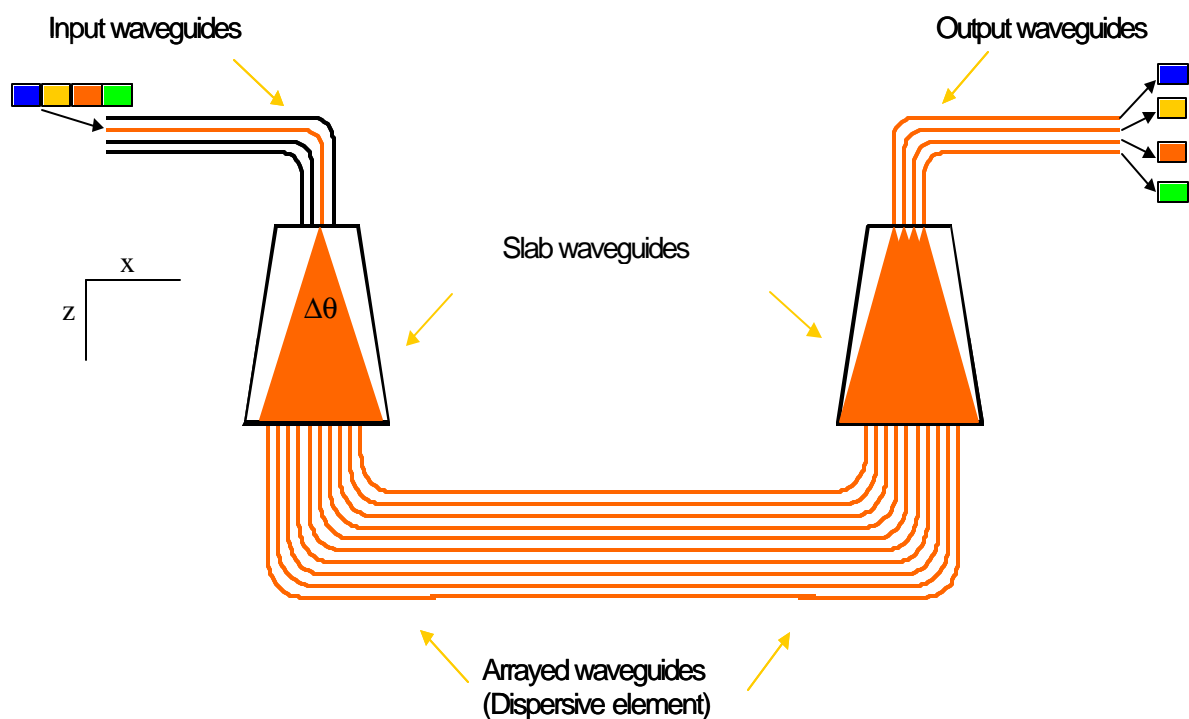


Figure 7.1: Block diagram for AWG

The AWG consists of input and output waveguides, two focusing slab regions (star couplers) that act as Fourier transform lenses [2] and a phase-array of multiple channel waveguides. Light propagating in the input waveguide is coupled into the array via the first coupler, as shown in Fig. 7.2 on page 102. The colours in this figure represent the normalized optical power of the light propagating through the star coupler. The light is diffracted where the input waveguide meets the slab waveguide because there is no confinement of the light in the horizontal plane. The diffraction pattern is simply the Fourier transform of the electric field at the input aperture of the slab

waveguide [3]. The angular spread, on the assumption of a uniform field, is given by $Dq = 2I_0/nW$ [4], where W is the width of the waveguide in the x -direction (see figure 7.1), and n is the effective refractive index of the slab. For $I_0 = 1.55\mu\text{m}$, $n = 1.48$ and $W = 5\mu\text{m}$ we calculate $Dq = 0.42 \text{ rad} \approx 24^\circ$. To preserve uniformity in power across the arrayed waveguides, one would normally use only a fraction (say 40%) of Dq .

The waveguide grating array samples the far field like a multi-slit aperture. The array has been designed such that (for the central wavelength of the multiplexer/demultiplexer) the optical path length difference between adjacent array arms equals an integer multiple of the centre wavelength of the multiplexer/demultiplexer. A position-dependent delay is added by the different lengths of the grating arms that make the angle of propagation into the second slab coupler wavelength dependent. The result is that the focal point in the image plane will be shifted away from the centre according to the wavelength of the component. Placing the output waveguides at these focal positions in the image plane allows separation of the desired wavelength channels [1, 2].

Figure 7.3 (on the next page) is a graphical representation of this process (for a certain wavelength). Once again, the colours in this figure represent the normalized optical power of the light propagating through the star coupler. Furthermore, the pathway monitor clearly shows how only output port 5 is excited by the input signal for this example.

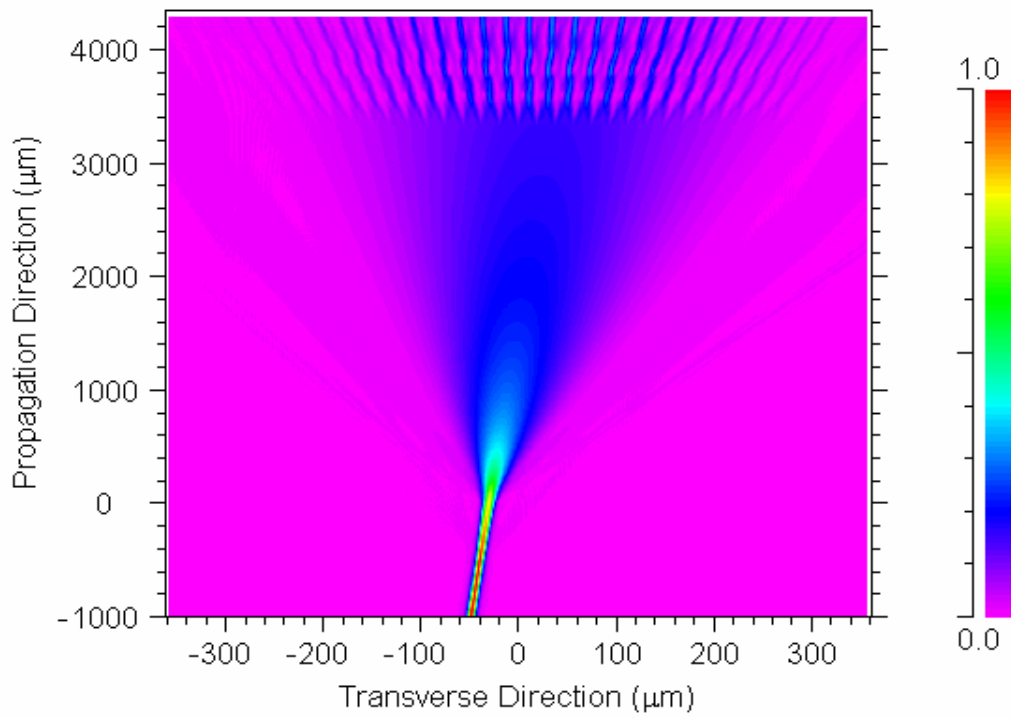


Figure 7.2: BPM simulation of light propagating through input star coupler

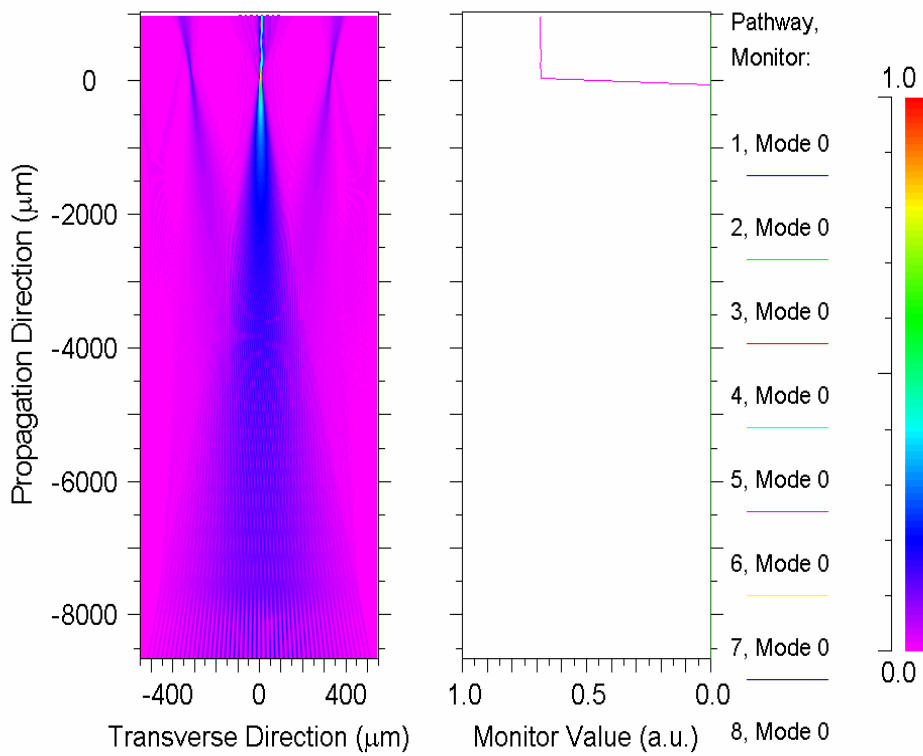


Figure 7.3: BPM simulation of light propagating through output star coupler

7.2) Star coupler layout

The lens element that constitutes the body of the input star coupler is constructed from the Rowland circle geometry as shown in figure 7.4. The design is identical for the output star, except that the light will be incident on the arc swept by R_o and not R_i . The body of the star coupler is formed between arcs AD and BC, and lines AB and DC. The indicated geometrical distances are parameters used by BeamPROP for circuit layout purposes. For a source on the Rowland circle, the diffracted waves focus at points on the Rowland circle. The proof is obtained by showing that the path length difference between a point source on the circle and two adjacent points on the grating (arc AD) is a constant equal to $d \sin \theta$ with d being the grating pitch [2]. The proof can be found in the appendix with a discussion on its applicability to AWGs. Although not clear from figure 7.4, the arc AD allows for almost straight focus lines, which is convenient for attaching a linear fibre or detector array.

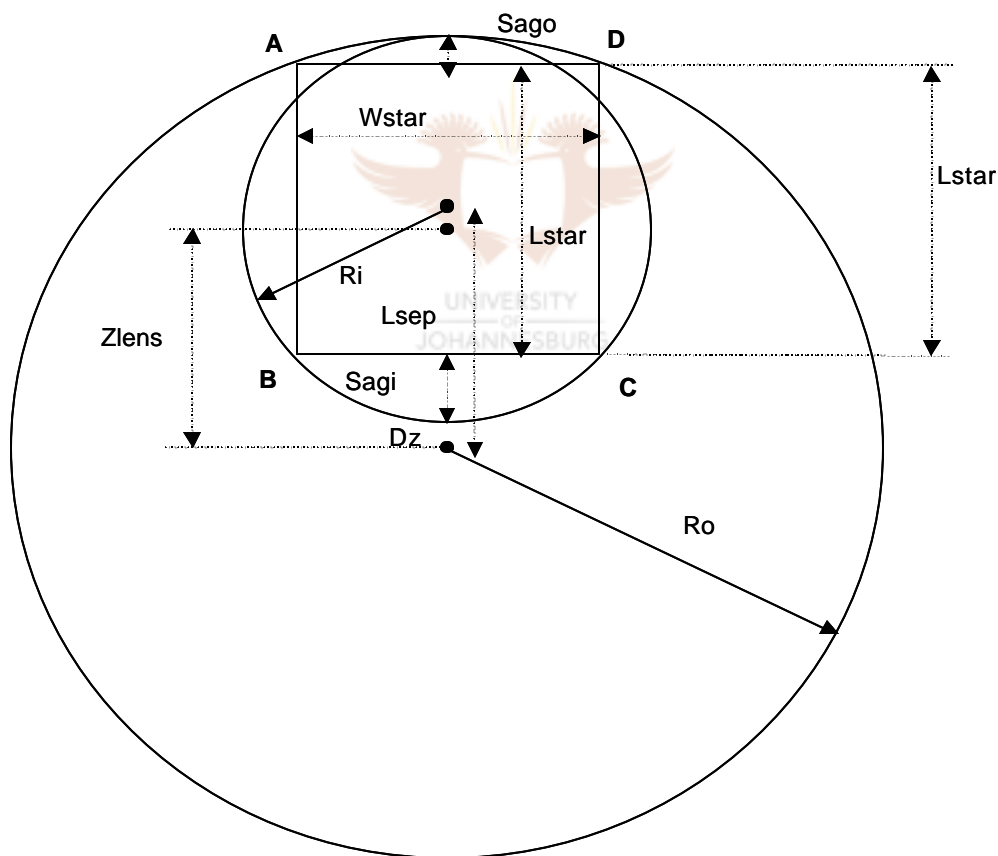


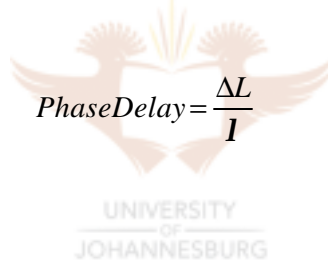
Figure 7.4: Rowland circle geometry for star coupler design

7.3) Theoretical derivation

As was stated earlier, the AWG consists of input/output waveguides, two focusing slab regions and a phase-array of multiple channel waveguides with the constant path length difference DL between neighbouring waveguides. We define the input waveguide separation in the first slab region as D_1 , the array separation d_1 and the radius of curvature f_1 [1]. In order to be general, it is assumed that the waveguide parameters in the first and second slab regions are different. Hence, the output waveguide separation is D_0 , the array separation d and the radius of curvature f_0 .

The input light is radiated to the first slab and then excites the array of waveguides. The amplitude of the excited electric field in each array waveguide is given by A_i , with $i = 1 - N$ (N being the total number of array waveguides). The amplitude profile of A_i is assumed to be a Gaussian distribution [1, 5]. As the light enters the second slab region after travelling through the arrayed waveguides (remember the DL), the beams interfere constructively and focus at the point x . The location of the focal point is dependent on the signal wavelength since

$$PhaseDelay = \frac{\Delta L}{\lambda} \quad (7.1)$$



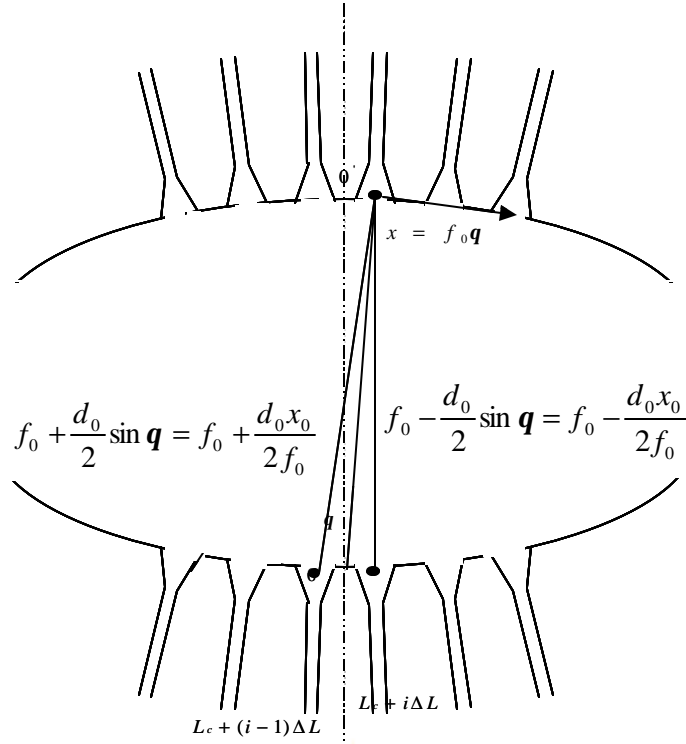


Figure 7.5: Enlarged View of Second Star Coupler

Figure 7.5 shows an enlarged view of the second slab region. The phase delays for the two light beams passing through the $(i - 1)$ th and i th array waveguides will now be considered. The distances of two beams are shown as approximated in figure 7.5. The difference of the total delays of the two beams must be an integer multiple of $2\mathbf{p}$ to enable constructive interference at focal point x_0 . The interference condition is given by

$$\begin{aligned}
 & \mathbf{b}_s(\mathbf{l}_0)\left(f_1 - \frac{d_1 x_1}{2f_1}\right) + \mathbf{b}_c(\mathbf{l}_0)[L_c + (i - 1)\Delta L] + \mathbf{b}_s(\mathbf{l}_0)\left(f_0 + \frac{d_0 x_0}{2f_0}\right) \\
 & = \mathbf{b}_s(\mathbf{l}_0)\left(f_1 + \frac{d_1 x_1}{2f_1}\right) + \mathbf{b}_c(\mathbf{l}_0)[L_c + i\Delta L] + \mathbf{b}_s(\mathbf{l}_0)\left(f_0 - \frac{d_0 x_0}{2f_0}\right) - 2m\mathbf{p}
 \end{aligned} \tag{7.2}$$

where \mathbf{b}_s and \mathbf{b}_c denote the propagation constants in the slab region and the array waveguide respectively, \mathbf{l}_0 is the centre wavelength of the WDM system, L_c is the minimum array waveguide length, and m is an integer. Simplification of equation 7.2 by subtraction leads to

$$\mathbf{b}_s(\mathbf{l}_0) \frac{d_1 x_1}{f_1} + \mathbf{b}_c(\mathbf{l}_0) \Delta L - \mathbf{b}_s(\mathbf{l}_0) \frac{d_0 x_0}{f_0} = 2m\mathbf{p} \quad (7.3)$$

When the condition

$$\mathbf{l}_0 = \frac{n_c \Delta L}{m} \quad (7.4)$$

is satisfied for the centre wavelength, the light at input position x_1 and output position x should satisfy the condition

$$\frac{d_1 x_1}{f_1} = \frac{d_0 x_0}{f_0} \quad (7.5)$$

The term n_c in equation 7.4 is an effective index of the array waveguide, whereas m is referred to as the diffraction order. Equation 7.5 is a very powerful one: it gives an output position x_0 for a known input position x_1 . It should be noted that $x_1 = x_0$ for most cases.

The dispersion of the focal position x_0 in terms of the wavelength and fixed input position is obtained by differentiating equation 7.3 with respect to \mathbf{l} . The result is

$$\frac{\Delta x}{\Delta \mathbf{l}} = - \frac{N_c f \Delta L}{n_s d \mathbf{l}_0} \quad (7.6)$$

where n_s is the effective index in the slab region and N_c the group index of the effective index n_c of the array waveguide ($N_c = n_c - \mathbf{l} \, dn_c/d\mathbf{l}$). The dispersion of the input position x_1 in terms of the wavelength for a fixed output position is given by

$$\frac{\Delta x_1}{\Delta \mathbf{l}} = \frac{N_c f_1 \Delta L}{n_s d_1 \mathbf{l}_0} \quad (7.7)$$

The input and output waveguide separations are $|x_1| = D_1$ and $|x_0| = D$ respectively. Substituting the abovementioned back into equations 7.6 and 7.7, and changing the subject of the equation to the wavelength yields

$$\Delta \mathbf{I}_{out} = \frac{n_s d_0 D_0 \mathbf{I}_0}{N_c f_0 \Delta L} \quad (7.8)$$

which is the wavelength spacing at the output side, and

$$\Delta \mathbf{I}_{in} = \frac{n_s d_1 D_1 \mathbf{I}_0}{N_c f_1 \Delta L} \quad (7.9)$$

which is the wavelength spacing at the input side. Generally, the parameters for the first and second slab regions are the same, so that:

- $D_1 = D_0$
- $d_1 = d_0$
- $f_1 = f_0$.

The conclusion is that $\Delta \mathbf{I}_{in} = \Delta \mathbf{I}_{out} \equiv \Delta \mathbf{I}$. The path length difference is obtained from either equation 7.8 or 7.9 as [1, 3]

$$\Delta L = \frac{n_s d_0 D_0 \mathbf{I}_0}{N_c f_0 \Delta \mathbf{I}} = m \frac{\mathbf{I}_0}{n_c} \quad (7.10)$$

The spatial separation of the m th and the $(m + 1)$ th focused beams for the same wavelength is obtained from equation 7.3:

$$\text{FSR} = x_m - x_{m+1} = \frac{\mathbf{I}_0 f_0}{n_s d_0} \quad (7.11)$$

where FSR represents the free spectral range of the AWG. Finally it is shown that the number of available wavelength channels N_{ch} is given by dividing the FSR with the output waveguide separation D as

$$N_{ch} = \frac{FSR}{D_0} = \frac{I_0 f_0}{n_s d_0 D_0} \quad (7.12)$$

7.4) Design specifications

Figure 7.5 shows a typical amplitude response of an 8×8 demultiplexer. The different colours denote the different output channels' wavelength response. Although the insertion loss, crosstalk and channel uniformity can be read off directly from this figure, it does not sufficiently describe certain other parameters, such as the accuracy of the channels to the international telecommunications union (ITU) grid. Furthermore, these parameters can be read off in various methods, for example at different wavelengths and with different references. The insertion of an optical component into an optical system leads to system degradation, which, in the case of an AWG, results in bit error rate degradation and reduced systems power [6]. It is thus imperative to analyse the AWG in a standardised manner and specifically in terms of the worst-case values.

A standardised way of analysing an AWG is by using the clear window method [6]. The “clear window” is defined as a band of wavelengths around each ITU centre wavelength. When quoting the performance of an AWG, all the specifications must be worst-case values met within the clear window of every channel [6].

UNIVERSITY
OF
JOHANNESBURG

Because the specifications are for the worst-case values, they are guaranteed for all the usable wavelengths defined by the window. Consequently, there is no need to calculate the effects of the passband shape, channel spacing error or polarisation because these variations are already accounted for in the specifications. The width of the window is chosen to be the range of wavelengths that the signal could occupy, accounting for the bandwidth of the signal drift in the wavelength of the laser. For 100GHz multiplexers, a window of 25GHz is typically used. Also, when noting the specifications of a single channel, the value should be for the worst case.

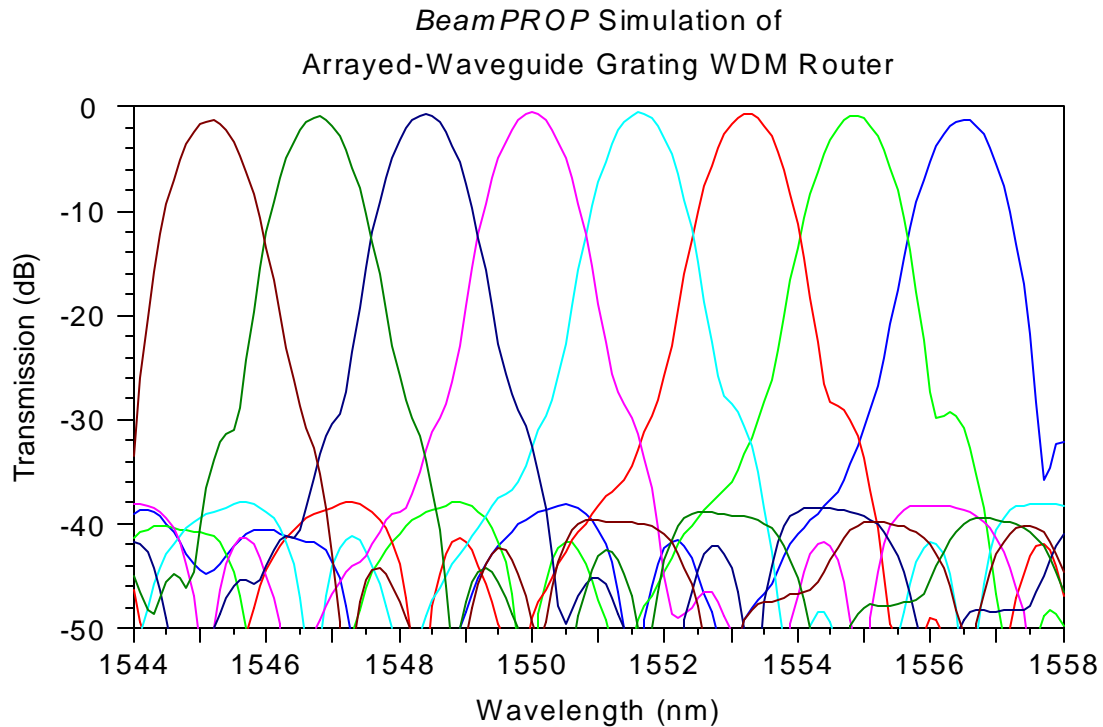


Figure 7.5: Typical amplitude response of an AWG

The following definitions should be applied to the characterisation of an AWG [4]:

- 1) The insertion loss is the minimum transmission within any clear window for all polarisation states.
- 2) The channel uniformity is the difference between the insertion losses of the best case and worst case.
- 3) The polarisation-dependent loss (PDL) is the maximum that the transmission can vary over all polarisations at a fixed wavelength, and over the entire clear window.
- 4) The passband uniformity is the maximum that the transmission can change with both polarisation and wavelength within the clear window of a selected channel.
- 5) The crosstalk is the highest transmission within a clear window that is referenced to the lowest transmission within the selected channel clear window. These include adjacent and non-adjacent crosstalk.

The above five characterisations can be applied to simulated AWGs. The reference [6] supplies additional measurements for characterisation of manufactured AWGs. Unless stated otherwise, the above procedure is used in the characterisation of the simulation results.

7.5) AWG design procedure

As can be seen from the previous theoretical derivation, there are many degrees of design freedom for AWGs. The main design requirements for an AWG are the channel spacing, passband width, cross-talk, loss and loss uniformity, and the number of output channels. In general, one must start with the definitions of the general waveguide structure [7], i.e. the width w and lateral V parameter is fixed. The subsequent steps in the design procedure are:

- 1) Receiver spacing d_r : For a safe design crosstalk level of -40 dB, the ratio of d_r/w is read off a numerical solution supplied in [7].
- 2) For a cyclical rotation of the input frequencies along the output ports, the free spectral range becomes (where Δf is the frequency channel spacing) [7]

$$FSR = N_{ch} \Delta f \quad (7.13)$$

- 3) Because of the above requirement, the required path length difference becomes

$$\Delta L = \frac{c}{n_g N_{ch} \Delta f} \quad (7.14)$$

where n_g denotes the group index as shown in section 6.5.2. With the above selection of FSR the loss uniformity will be set at ± 3 dB. This is explained by noting that channels that are at frequency $FSR/2$ away from the central frequency receive equal amounts of power resulting from the two orders that focus symmetrically around the centre image plane. Because of the periodical design, the frequency spacing between the outer channels comes close to the FSR, resulting in the 3dB loss.

- 4) The divergence angle is calculated from

$$\Delta \alpha = \frac{n_g \Delta f \Delta L}{n_{star} f_0 d_r} \quad (7.15)$$

where n_{star} is the refractive index of the star coupler region.

- 5) The length of the star region (R) is obtained from equation 7.15 by selecting an appropriate array spacing, and using the relation $\Delta a = d_a/R$, where d_a is the array spacing.

- 6) The number of output arrays is chosen such that the array will completely cover the divergence region. This number sets the angular half width of the array aperture.

This completes the design procedure from a purely theoretical viewpoint. When circuits are designed in BeamPROP, two central design equations can be used

$$grating_order = \frac{I_0}{N_{ch} \Delta I} \quad (7.16)$$

where I_0 is the centre design wavelength and ΔI is the channel spacing. Also

$$R = \frac{n_{star} d_r d_a}{grating_order \cdot \Delta I} \quad (7.17)$$

where n_{star} is the index of the star coupler region, and d_r is the receiver spacing as discussed on the previous page. Equation 7.17 differs from design step 4 as given above in that it takes the number of wavelength channels into account, resulting in an indirect calculation of equation 7.15. The width of d_a should be chosen so as to minimise the total loss of the circuit according to [7]

$$L_0 \approx 17 e^{-4p v_c^2 / d_a^2} \quad (7.18)$$

When designing an AWG in BeamPROP, the parameters defined in the beginning are the centre wavelength (I_0), the channel spacing (ΔI), the number of wavelength channels (N), the number of input and output channels, and the number of waveguides in the array (M). The number of wavelength channels is chosen to be between 1.5 and 2 times the number of input/output waveguides, since the demultiplexing loss increases in the peripheral output ports of the AWG [8].

7.6) BPM simulation of AWG

A 50GHz (0.4nm) AWG router was designed for communication purposes utilising the waveguide parameters as set out in chapter 4. Because the spot sizes that affect the working of the AWG are in the xplane, we can readily use a two-dimensional simulation, which reduces the computation time (BeamPROP allows for 3D simulations of AWGs, but this procedure is extremely slow and seemed unstable). A width of $3\mu\text{m}$ cannot be used, however, because the slab structure used in the three-dimensional case leads to a slightly larger mode

field radius than for a pure two-dimensional case. A 2-D waveguide width of $5\mu\text{m}$ emulates the mode field radius of $3.1\mu\text{m}$ as supplied in section 4.2, and is subsequently used in the simulations. The design parameters for the AWG are as follows:

Centre wavelength λ_c	1550nm
Channel spacing $\Delta\lambda$	0.8nm (100GHz)
Number of waveguides in array	121
Input/output channels	16
Wavelength channels	32
Star length R	13831.97 μm
Path length difference	63.25 μm
Grating order	81
Free spectral range	0.02 μm

Table 7.1: Design parameters for communications AWG

The BPM simulation for a TE polarisation is presented in figure 7.6, and for TM polarisation in figure 7.7. The AWGs are designed such that the centre 8 channels are to be used. With this in mind, the results from the simulations are presented in Table 7.2.

Passband width (3dB)	0.3nm
Adjacent crosstalk	15.5dB
Non-adjacent crosstalk	26dB
Minimum insertion loss	3.4dB
Insertion loss uniformity	1.84dB
Polarisation dependent loss (PDL)	0.2dB

Table 7.2: AWG results summary

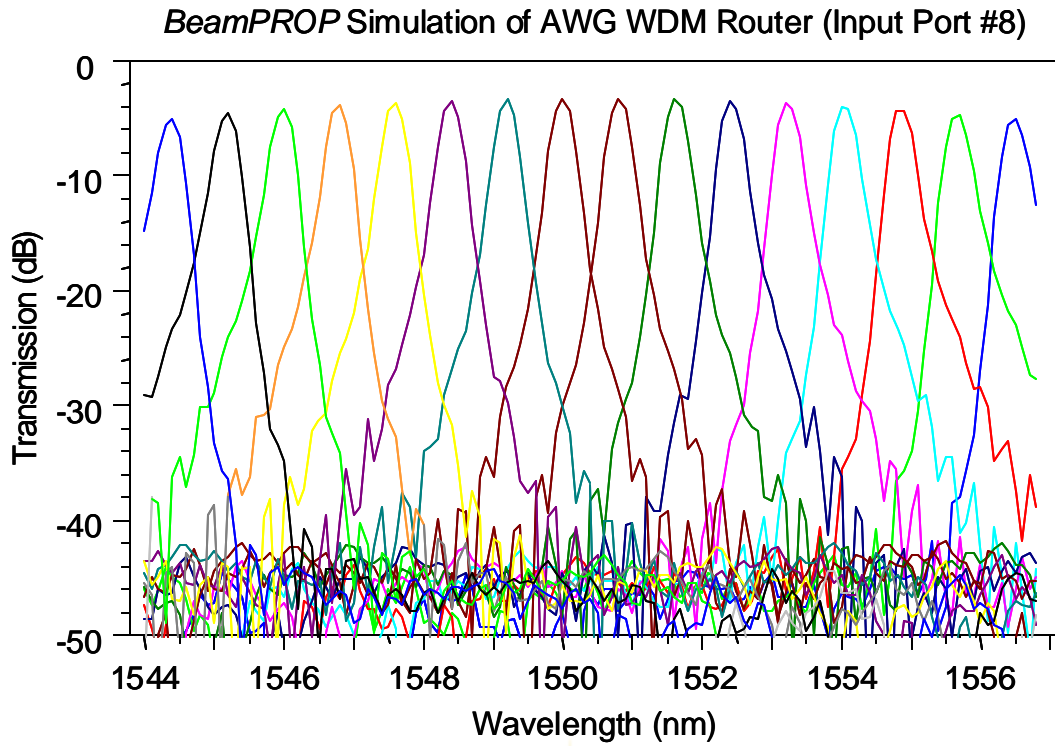


Figure 7.6: BPM simulation results for TE mode

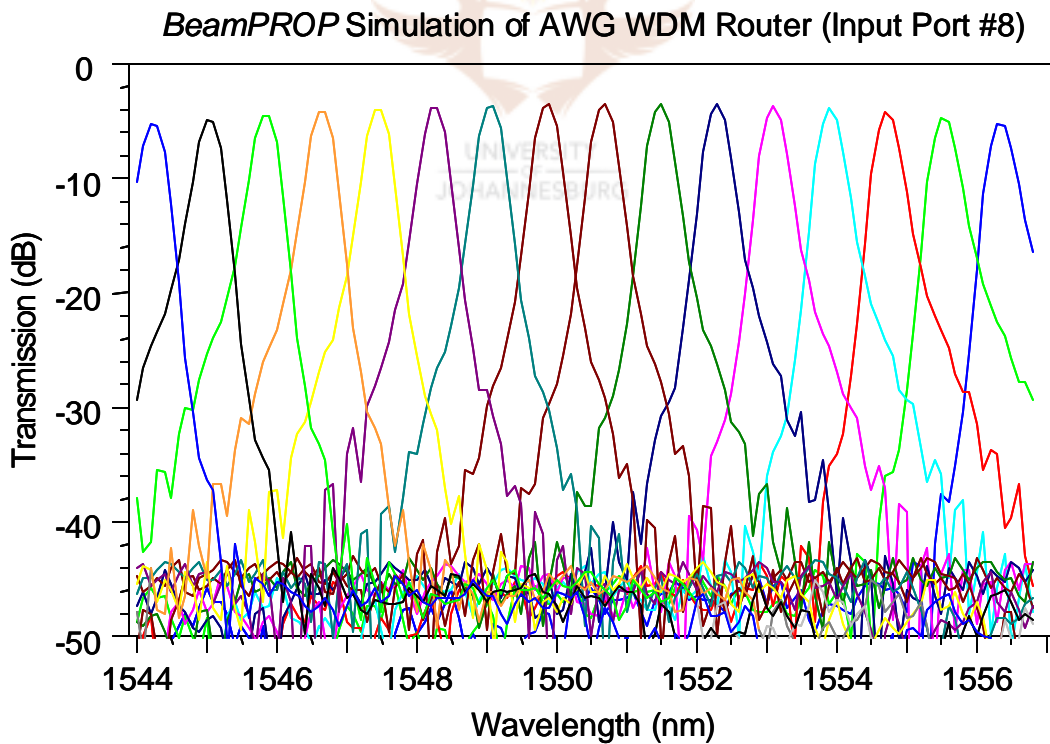


Figure 7.7: BPM simulation results for TM mode

The results compare well with specifications for manufactured AWGs. The design can be optimised slightly in many ways. For example, if a narrower passband is desired, a straightforward way of doing this is to increase the number of waveguide gratings [9]. Loss can also be reduced by trading for a decrease in FSR while maintaining the same channel spacing [9]. This is done by increasing the angle between outputs.

As a final note, the AWG was simulated for a width of $5\mu\text{m}$, whereas the design in chapter 4 had a width of $3\mu\text{m}$. The physical layout for the AWG before patterning is done for the width of $3\mu\text{m}$, while maintaining the designed array separation of $15\mu\text{m}$ and input/output separation of $20\mu\text{m}$, and increasing the taper length slightly to keep the width at the slab interfaces the same as for the simulated case.

7.7) AWGs in laser applications

AWGs can be used in the realisation of multi-frequency lasers (MFLs). MFLs are attractive components since they can simultaneously deliver many densely spaced optical wavelength channels, each of which can be modulated individually [10]. An important characteristic of MFLs is that the relative channel spacing is defined by the geometry of the intracavity AWG, and is therefore stable and reproducible [10]. MFLs are formed by integrating semiconductor optical amplifiers (SOAs) in the input and output waveguides (only one input waveguide is realised).

The main trade-off to consider when designing an AWG for the purposes of MFL implementation is between the number of arrayed waveguides and the length of the FSR. Firstly, the filter bandwidth of the intracavity AWG should be as narrow as possible. A narrow filter bandwidth guarantees that the laser locks on a single longitudinal mode regardless of how many longitudinal modes are contained in that filter bandwidth [11]. Secondly, the FSR of the AWG should be as large as possible so that the selectivity of the amplifier gain profile is sufficient to choose lasing in only one passband of the AWG [11]. By chirping the router, multi passband lasing can be suppressed, leading to a relaxation of the aforementioned tradeoffs.

7.7.1) Chirping of AWGs

Chirping the grating arm lengths (i.e. by adding varying extra length to existing grating arms to the physical structure according to a required extinction requirement, as is discussed further on) of the AWG can cause the transmissivity of the component to have one dominant passband around the

centre wavelength, with the peak transmissivities in adjacent grating orders suppressed [9]. This suppression is useful for controlling the oscillation frequencies of multi-frequency AWG lasers and reducing the spontaneous emission beat noise in preamplified AWG receivers [12]. Chirping only the arm lengths causes an increase in passband for the outputs (except 1) and an increase in the loss non-uniformity. By chirping the angular distribution of the waveguides at the slab interfaces, these constraints are eliminated.

Following [9], the chirping of the arm lengths and angular distributions are derived to be:

$$L(m) = \text{round} \left\{ \left[m + g(m) \right] \frac{\Delta L b_c}{2p} \right\} \frac{2p}{b_c} + \text{const.} \quad (7.19)$$

$$\mathbf{a}(m) = \Delta \mathbf{a} \left(\text{round} \left\{ \left[m + g(m) \right] \frac{\Delta L b_c}{2p} \right\} \frac{2p}{\Delta L b_c} - \frac{M+1}{2} \right) \quad (7.20)$$

where $L(m)$ is the grating arm length, $\alpha(m)$ is the angle between the input waveguide and star coupler, ΔL is the constant path length difference, β_c is the propagation constant for the centre wavelength, $\Delta \alpha$ is the angular spacing between the grating waveguides if the star coupler is unchirped and $g(m)$ is an arbitrary function.

The function $g(m)$ should be chosen so as to provide a large and consistent extraneous passband extinction ratio. Such a $g(m)$ is given in [7] as:

$$g(m) = \mathbf{g} \left(\left[\frac{m - \frac{M+1}{2}}{1 - \frac{M+1}{2}} \right]^2 - \frac{1}{3} \right) \quad (7.21)$$

Equation 7.21 is referred to as the parabolic chirp. It corresponds to a linear increase in increment, and so to have the highest transmissivity the grating waveguides at the array free-space region should get wider when $\mathbf{g} > 0$ and smaller when $\mathbf{g} < 0$ (from the shortest to the longest arm).

The term $-1/3$ in equation 7.21 was found empirically. It maximises the overlap of the effective modes in the grating arms from the star couplers [9]. In the simulations that are presented a singular chirp of path length is presented, as work is still being done on the double-chirping simulations. A MATLAB program was written by employing equations 7.19 and 7.20 to calculate the required additional path lengths. The program can be found in the appendix. The design parameters for the proposed laser application AWG are given in table 7.3.

Centre wavelength λ_c	1560nm
Channel spacing $\Delta\lambda$	0.8nm (100GHz)
Number of waveguides in array	101
Input/output channels	8
Wavelength channels	16
Star length R	3073.77 μm
Constant path length difference	127.31 μm
Grating order	122
Free spectral range	12.9nm

Table 7.3: Design parameters for laser application AWG

The BPM simulation results for the unchirped and chirped AWGs are presented in figures 7.8 and 7.9 respectively. It is clear how the passbands in the adjacent FSR centres are attenuated for the chirped case. An attenuation coefficient of $g = 4$ was used to generate the chirping lengths, resulting in an average sideband extinction of 7.34dB. The results are presented in table 7.4.

	Chirped	Unchirped
Minimum insertion loss	0.8dB	1.04dB
Channel uniformity	3.9dB	1.56dB
Crosstalk	35dB	35dB

Table 7.4: Chirped vs. unchirped AWG results summary

The crosstalk result from table 7.4 does not entirely agree with the theory, where it is expected that the crosstalk should be smaller for the chirped case. This can be explained by looking at the

channel width of the unchirped AWG, which results in neither a clear adjacent or non-adjacent crosstalk, but the noisy crosstalk seen in figure 7.8. Because this crosstalk is not clearly discernable, the improvement for the chirped case is not obvious.

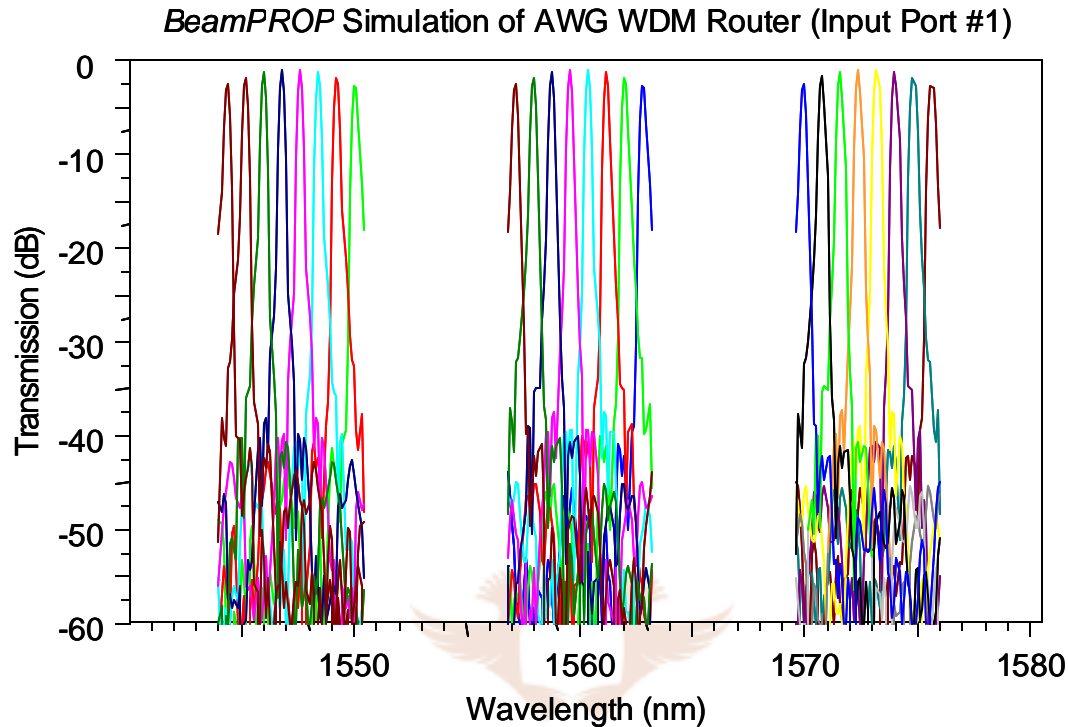


Figure 7.8: BPM result of unchirped AWG over three periods

In [9], the empirical requirements for an MFL-AWG are given as $FSR > 15\text{nm}$ and channel spacing of 50GHz . By chirping the component, the above constraint is relaxed [9]. The presented chirped AWG has a passband of 0.7nm at -25dB for the centre channel, thus meeting the 50GHz constraint. Because of the suppression of the sidebands, the FSR of 12.9nm is also sufficient. By double chirping the component, all the required passbands can meet the required width.

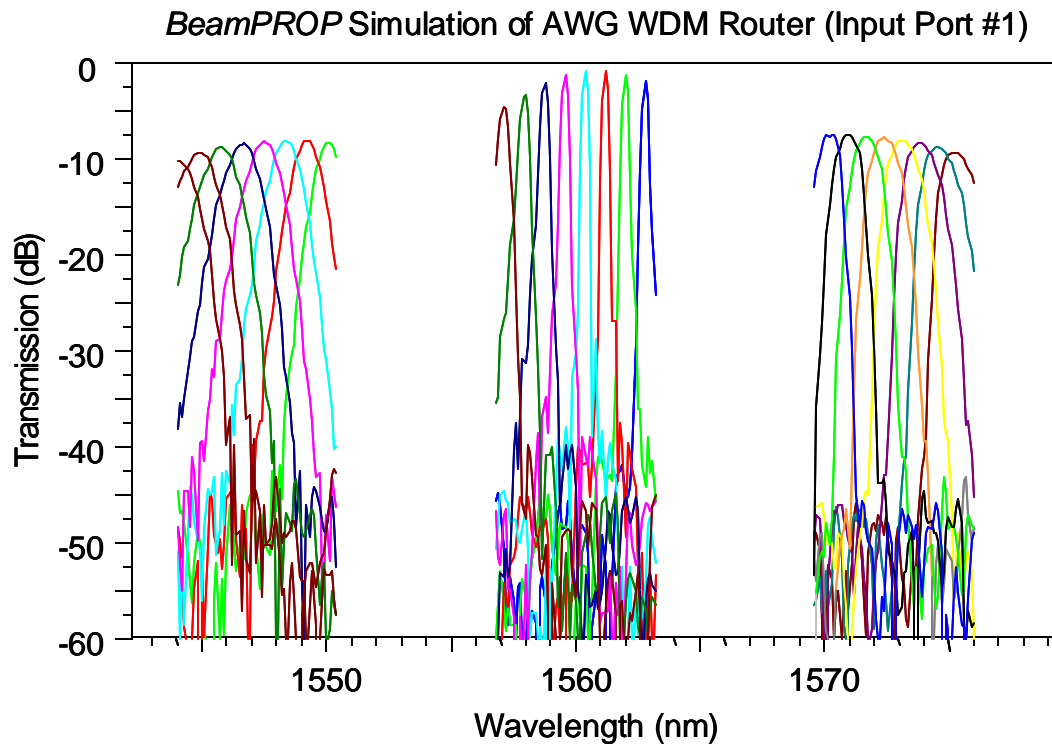


Figure 7.9: BPM result of chirped AWG over 3 periods

7.8) Conclusions

AWGs are versatile and highly integrated PLCs that are used for multiplexing and demultiplexing signals. They can also be used in multifrequency lasers

Another important application of AWGs is in the area of signal processing. So, for example, second- and third-order dispersion compensation can be achieved by introducing a spatial filter to the demultiplexed signal and reflecting this rectified spectrum back through the AWG, as depicted in figure 7.10. The reader is referred to [5, 13] for further reading regarding this application.

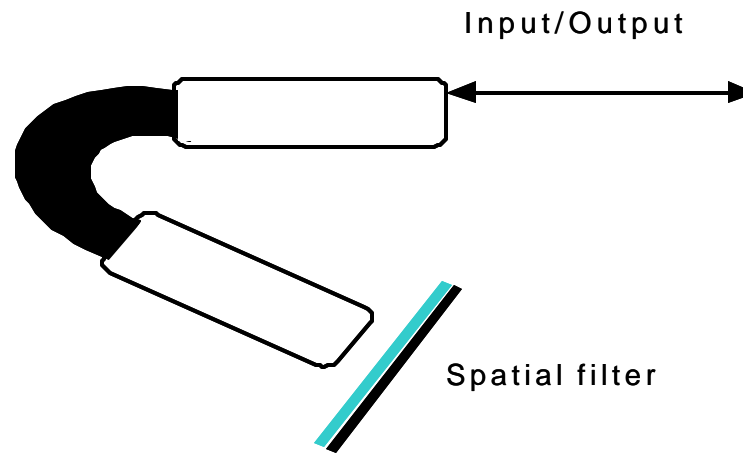


Figure 7.10: Application of AWG as dispersion compensator

AWGs can also be used in OADM configurations by simply dropping and adding wavelength channels at designated nodes. Finally, AWGs can be used as powerful tuneable filters as reported in [13].



7.9) References

- 1) K Okamoto, "Recent progress of integrated optics planar lightwave circuits", *Optical and Quantum Electronics*, vol.31, pp. 107 - 129, 1999.
- 2) C.K. Madsen, J.H. Zhao, "Optical filter design and analysis: A signal processing approach", Wiley interscience, 2000.
- 3) B. Saleh, M. Teich, "Fundamentals of photonics", Wiley Interscience, First edition, 1991.
- 4) D. Lee, "Electromagnetic principles of integrated optics", Wiley Interscience, First edition, 1986.
- 5) H. Takenouchi, H Tsuda, "Analysis of optical-signal processing using an arrayed-waveguide grating", *Optics Express*, vol. 6, pp. 124 – 135, 2000.
- 6) M. Volanthen, M. van der Vliet, V. Tandon, J. Bonar, "Characterisation of arrayed waveguide gratings: White Paper", BMKGF –01000 00, Kymata Ltd., 2001.
- 7) M. Smit, C. van Dam, "PHASAR-based WDM-devices: principles, design and applications", *IEEE Journal of Selected Topics in Quantum Electronics*, vol.2, pp. 236 – 250, 1996.

- 8) K. Okamoto, A. Kaneko, M. Itou, "Array waveguide grating routers for 50GHz applications", OFC 1999 technical journal, TuN1-1, pp. 190 – 192, 1999.
- 9) C. Doerr, C. Joyner, "Double-chirping of the waveguide grating router", IEEE Photonics Technology Letters, vol. 9, pp. 776 – 778, 1997.
- 10) C. Doerr, C. Joyner, L. Stulz, J. Centanni, "Wavelength selectable laser with inherent wavelength and single-mode stability", IEEE Photonics Technology Letters, vol. 9, pp. 1430 – 1432, 1997.
- 11) M. Zirngibl, C. Joyner, C. Doerr, L. Stulz, H. Presby, "An 18-channel multifrequency laser", IEEE Photonics Technology Letters, vol. 8, pp. 870 – 872, 1996.
- 12) C.R. Doerr, C.H. Joyner, M. Zirngibl, L.W. Stulz, H.M. Presby, "Polarization diversity waveguide grating receiver with integrated optical preamplifiers", IEEE Photonics Technology Letters, vol. 9, pp. 85 – 87, 1997.
- 13) M. Zirngibl, C. Joyner, B. Glance, "Digitally tunable channel dropping filter/equalizer based on waveguide grating router and optical amplifier integration", IEEE Photonics Technology Letters, vol. 6, pp. 513 – 515, 1994.

